# Probing the Surface $T_g$ of Monodisperse PS by Local Thermal Analysis

**Hartmut Fischer***

*TNO TPD Innovative Materials, P.O.B. 595, 5600 AN Eindhoven, The Netherlands, c/o TU Delft, Faculty of Aerospace Engineering, Kluyverweg 1, 2629 HS Delft, The Netherlands*

*Received August 5, 2004; Revised Manuscript Received November 15, 2004*

ABSTRACT: The surfaces of compression-molded PS samples with different $M_w$ (9.85 kg/mol−502 kg/mol) and narrow molecular weight distributions were examined using an AFM equipped with a thermal probe in the local thermal analysis (LTA) mode to get further insight into possible explanations of a decrease in glass transition temperature ($T_g$) at polymer surfaces. No difference in $T_g$ at the very surfaces could be detected for these samples. Instead, different molecular weights contribute to differences in the micro-thermomechanical behavior. A careful analysis hints to possibilities to use this analytic method for the determination of $M_w$ and/or molecular weight distribution on polymeric surfaces. Furthermore, hints to a disentanglement of macromolecules with molecular weights lower than the critical molecular weight to form a random coil, initiated by the indentation with the thermal probe during the LTA experiment, are found.

## Introduction

The phenomenon of glass transition at temperature $T_g$ in polymers is still an interesting and frequently discussed topic in polymer science. Many important characteristics, mainly the rheological and mechanical behavior of polymers, are connected and can be correlated to the $T_g$. In general, the glass transition is related to cooperative motion dynamics of parts of polymer chains controlled by an intrinsic length scale of the order of a few nanometers (~3 nm). The size of that length scale is temperature-dependent. The behavior of polymers changes rigorously while crossing the $T_g$. Polymers are hard and glassy at temperatures below $T_g$ and soft and rubbery for temperatures above $T_g$. The glass transition temperature $T_g$ is a function of the molecular weight of polymers and can be described by a simple equation:

$$T_g = T_{g\infty} - \frac{K}{{M_n}^{\gamma}} \qquad (1)$$

where $T_{g\infty}$ is the $T_g$ of infinite molecular weight, $K$ is constant equal to the critical molecular weight where molecules start to behave like polymers, and $M_n$ is the number-average molecular weight.

The equilibrium $T_g$ is reached when the polymer chain exhibits the conformation of a statistical coil, and an entanglement of random coils is observable and is therefore dependent on the $M_w$ and on the flexibility of the polymer chain. The equilibrium $T_g$ of polystyrene of a molecular weight higher than the critical value of about 100 kg/mol is about 105 °C.[1] The molecular weight dependency of the $T_g$ is well-known and reported elsewhere.[1−4]

However, polymers can display a lower $T_g$ at free surfaces. Since the origin of the depression of the glass transition temperature on air/vacuum−polymer interfaces is still a subject of intense research, the main visions, explanations, and theories concerning this subject will be discussed briefly. The principles of the layered model for the description of near surface layers with a lower $T_g$ than the bulk polymer as described by Jones[5] but also by Mattson et al.,[6] de Gennes,[7] and in general for materials by van der Veen[8] are shown in Figure 1.

A very thin layer of (liquid) polymer with a high mobility and with much lower density than the bulk material is proposed to exist at the very surface (thickness between 0.5 and 2 nm). This layer is supposed to be very flat and displays a roughness due to the period of capillary waves. Underneath this top layer, a layer of polymer (thickness 20−100 nm) with a reduced glass transition and increased mobility exists before the bulk material with the known bulk glass transition sets in.

A lower $T_g$ at polymer surfaces (Figure 1) may be caused by the following:

1. The excess free volume induced by surface enrichment of end groups which causes an enhanced mobility of chain segments and a lower polymer segment density (finite size effects).

2. A possible confinement of polymer chains for polymers with high $M_n$. Since the region of cooperative motion is only extended to a few nanometers, the break in symmetry at polymer surfaces (flattened chain conformation) or a chain confinement in films with $d < R_g$ will be able to alter conformation of chains and to decrease the number of interchain entanglements. In this case $T_g$ is expected to scale with $R_{EE}$, which will also result in a reduction in density (at the surface) by 5%!

3. Another explanation has been proposed by de Gennes,[7] which explains a lowering of the glass transition at polymer surfaces by collective motions along the chain (loop motions) which require a weaker free volume and does not involve chain ends. Loop motions, which are independent of chain length, win in the thin film case against standard motions, which are only controlled by the free volume as can be shown experimentally.[9]

4. Yet a possible explanation may be found by experiments and theory[10−13] which prove an enrichment of low molecular weight fraction at the surface. Those lower molecular weight fractions display a lower surface tension, and their location at the surface leads to a lower

---

* E-mail hfischer@tpd.tno.nl.

10.1021/ma048376a CCC: $30.25

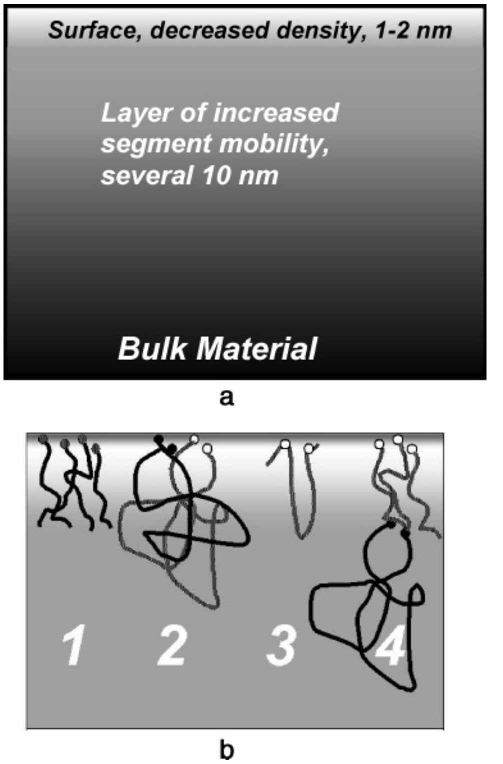

**Figure 1.** (a, top) Schematic picture of the surface of a glassy polymer showing a thin layer of reduced density at the surface followed by a layer of increased mobility of polymer segments changing smoothly to the bulk material. (b, bottom) Schematic pictures depicting possible mechanisms of lowering the $T_g$ close to surfaces: (1) excess free volume induced by surface enrichment of end groups which causes an enhanced mobility of chain segments and a lower polymer segment density, (2) confinement of polymer chains for polymers with high $M_n$ which causes break in symmetry at polymer surfaces (flattened chain conformation) and a chain confinements in films with $d < R_g$, (3) increased collective motions along the chain (loop motions) which require a weaker free volume and does not involve chain ends, (4) enrichment of low molecular weight fraction at the surface.

free energy due to a smaller change in conformational entropy, which initiates a phase separation in terms of molecular weight. The resulting surface layer will display a lower glass transition according to the already above-mentioned Flory−Fox equation (1).

There is a demand on contact mechanical experiments in the nanoscale region to contribute to the fundamental understanding of the glass transition.[14] In an earlier work,[15] the existence of a surface layer with a lower $T_g$ as well as the possible existence of the very thin layer of liquid polymer at the very surface has been successfully demonstrated using local thermal analysis and scanning thermal microscopy. However, this study has been performed on a PS sample with a molecular weight of about 300 kg/mol and a rather broad molecular weight distribution (3.5). Alternative determinations of glass transition temperatures in thin polymer films using local thermal analysis experiments on thin films of polystyrene (PS) and of poly(methyl methacrylate) (PMMA)[16] are described in the literature. Those experiments confirmed the earlier by ellipsometry,[17−19] Brillion light scattering,[20,21] positron annihilation spectroscopy,[22] SIMS,[23] lateral force microscopy,[24−27] and SFM[11] but also by simulations[28,29] found decrease in $T_g$ for PS with decreasing thickness of thin free-standing and/or supported films.

**Table 1. $T_g$ of the PS Samples Used for This Study As Calculated Using the Flory−Fox Equation (FF), As Determined by LTA (Scanning Speed 10K/s) and As Determined by DSC (Scanning Speed 10 K/min)**

| $M_w$ (kg/mol) | 9.85 | 23.5 | 50 | 101 | 214 | 288 | 502 |
|---|---|---|---|---|---|---|---|
| $T_g$ FF (°C) | 94.4 | 100.5 | 102.8 | 103.9 | 104.4 | 104.6 | 104.7 |
| $T_g$ DSC (°C) | 95 | 99 | 101 | 103.3 | 104.4 | 104.6 | 104.5 |
| $T_g$ $\mu$-TA (°C) | 118 | 120 | 123 | 122.5 | 122.6 | 122.5 | 122.5 |

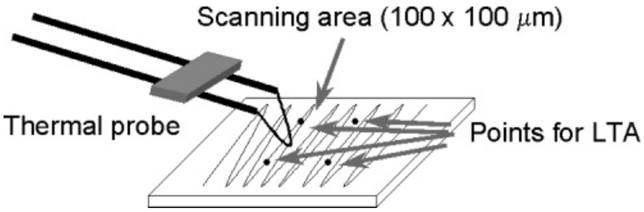

**Figure 2.** Schematic setup of the local thermal analysis experiments (LTA). The LTA experiments were performed in contact mode between 0 and 300 °C at four different locations on a 100 × 100 $\mu m^2$ scan at least at three different areas using heating speeds of 10 K/s. The different symbols are only used for a discrimination of the different data derived from the different samples; the real data point density is 2/K.

In all of these studies the above-mentioned ideas about the origin surface layers with lowered $T_g$ are discussed.

The present study was performed on PS samples with a narrow molecular weight distribution and $M_w$'s between 9.8 kg/mol and 502 kg/mol by LTA in order to discriminate between the possible explanations of the origin of a lower $T_g$ at polymer surfaces.

## Experimental Section

PS samples with narrow molecular weight distribution ($M_n$ = 9.85, 23.5, 50, 101, 214, 288, and 502 kg/mol, $M_n/M_w$ = 1.02−1.05) were purchased from polymer standards. Additional to that another sample, a commercially available PS (Styron 634, Dow Chemical) with a broad molecular weight distribution ($M_n$ = 78 kg/mol, $M_n/M_w$ = 3.6) was inspected. The $T_g$ of the samples was determined macroscopically between 50 and 200 °C using a conventional DSC (Perkin-Elmer PYRIS, heating speed 10 K/min; see Table 1). The samples were prepared by compression-molding of 2 mm thick plates under nitrogen at 120 °C against freshly cleaned float glass surfaces and splitting them off after cooling. The scanning thermal microscope (SThM) used in this study was a Micro-Thermal analyzer ($\mu$TA 2990) from TA Instruments. Local thermal analysis was performed between 0 and 300 °C at four different locations on a 100 × 100 $\mu m^2$ scan (see Figure 2) and at least at three different areas using heating speeds of 10 K/s; 20 data points were collected per second.

The calibration of the thermal sensor was carried out following known procedures. The probes have a spring constant of about 5−10 N/m. The contact surface area between probe and substrate (ca. 2−6 $\mu m^2$) was determined by inspection of the mark of the probe left on the substrate after a short contact (1−2 s) at 100 °C. Different contact forces ranging between 20 and 60 nN resulting in a contact pressure of about 5−10 kPa were used. The dependency of the $T_g$ on pressure in PS is small and has been reported as $dT_g/dP = 2.5 \times 10^{-7}$ K/Pa,[30] which translates into a change in $T_g$ of less than 0.1 K for the force range applied by the probe tip.

**Instrumentation and Methods.** The scanning thermal microscope (SThM, $\mu$-TA) combines the visualization possibilities of the atomic force microscopy (AFM) and its ability to image topography, phase shifts, friction, stiffness, and adhesion with the characterization capabilities of thermal analysis (thermal conductivity, micro-differential thermal analysis, and micro-thermomechanical analysis) in a single instrument.[31] The scanning mode may be used for the inspection of surfaces with respect to their thermal properties using a scanner with

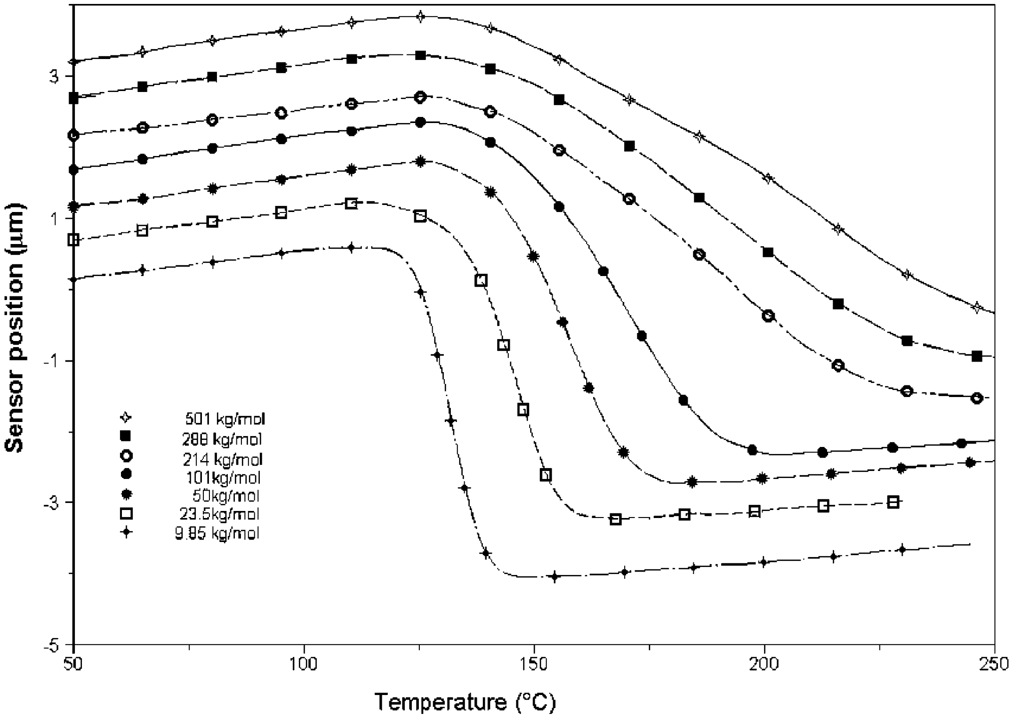

**Figure 3.** Results of the LTA experiments performed on surfaces of PS samples with different molecular weight. Plotted is the sensor position with respect to temperature. The change in slope represents the $T_g$; the slope after crossing the $T_g$ can be related to the melt viscosity.

a thermal sensor as probe (tip). A second mode gives the option to perform a local thermomechanical analysis of discrete areas of a few square microns (L-TMA and L-CA), currently a generally accepted method for the determination of $T_g$'s of surfaces.[31]

A few aspects, however, should be discussed in more detail. The thermal probe acting as heater, height, and thermal sensor at the same time detects during heating in contact mode the sensor position and the heat flow to the sample. Any thermodynamic phase transition connected with a change in mechanical properties (softening, expansion, melting) and thermal properties (heat of fusion, change of heat capacity) will thus be detected by both methods. Anyway, a glass transition is connected with only small changes in heat capacities. Therefore, for the detection of glass transition temperatures more often the point is been used when the sensor penetrates the sample due to softening while crossing over the $T_g$ (thermomechanical analysis, TMA). In a TMA experiment a probe is lowered onto the surface of a sample and the movement of the probe is measured as the sample is heated. With a load applied to the probe, a combination of modulus changes and expansion of the sample are observed. Depending upon the probe/sample contact area and the load applied, the $T_g$ can be detected by either an upward (expansion) or downward (penetration) movement of the probe. With large contact areas and very low forces expansion is primarily observed, whereas for smaller contact areas and/or higher forces penetration is primarily observed. The location of this point is however rather connected to changes in melt viscosity and the thermomechanical response at a certain contact pressure than by the thermal effect itself. That makes a precise detection difficult and very dependent on the molecular weight of the polymer sample since the melt viscosity scales with the molecular weight at a power between 3 and 5! Furthermore, the large probe size used currently in the scanning thermal microscopy (ca. 2−5 $\mu m^2$) and the low spring constants of the cantilevers result in rather low contact pressures (5−15 kPa) which may not be sufficient to cause an instant thermomechanical response, especially at samples with a high melt viscosity. Also, since the local thermal analysis uses rather high heating rates (5−20 K/s), a delay in time/temperature of thermomechanical effects may have to be expected, especially for polymers with a low heat conductivity value. In addition to that, changes of the contact area between probe and sample with increasing penetration depth during the local thermal analysis will lead to an influence onto the quality of the pure thermal signal, which has to be taken into account. The heating rate also has an effect on the detection of $T_g$ similar to macroscopic experiments. As the heating rate is reduced, the sensor deflection at $T_g$ is increased, the signal-to-noise ratio is decreased, and the transition temperature is shifted downward. However, the precision of temperature measurement appears to be somewhat dependent upon heating rate at the very fast rates typically employed with $\mu$TA. Heating rates between 10 and 25 K/s (i.e., 600 and 1500 K/min) give consistent results for the $T_g$ detection and are therefore recommended by the instrument constructors,[32] while those at lower rates between 2 and 8 K/s (120 and 480 K/min) are described to display substantially poorer precision. This explains the shift of the transition temperatures upward toward higher temperatures than those detected by "classical" DSC experiments (see Table 1) and those calculated using the Flory−Fox equation with known parameters ($T_{g,\infty} = 104.9$ °C, $K = 1.14 \times 10^5$).[1]

Only the thermomechanical signal (sensor position) has been used for the detection of $T_g$ due to the reasons mentioned above (see Figure 3).

## Results and Discussion

First, it was observed that the main transition ($T_g$) occurred for all the samples for $M_w > 100$ kg/mol at approximately the same temperature (122−123 °C) and at somewhat higher temperatures, compared to the known 105 °C, due to the experimental conditions chosen as explained above. This rules a possible creation of low molecular weight fragments at the polymer surface by chain fragmentation of chains adhered to the glass surface during the sample preparation out. The data obtained are not at all surprising, since the molecular weight−$T_g$ relation, as expressed by eq 1, levels off for $M_w > 100$ kg/mol to a constant value. A $M_w$ value larger than 100 kg/mol seems to be rather high for molecules to behave like a polymer also since the average molecular weight between entanglement points $M_e$ for PS is about 17 kg/mol only. However, and as discussed below in detail, for PS only molecules with a molecular weight larger than 100 kg/mol behave truly as macromolecules. The three samples with lower $M_w$ show indeed a lower $T_g$; however, this is due to the above-mentioned molecular weight−$T_g$ relation rather than to surface-related effects. A very recent publication dealing with calorimetric experiments on thin films offers possible explanations for this discrepancy.[33]

The absence of a dependence of $T_g$ on the film thickness down to a few nanometers using a nanocalorimetric[33] technique is also contrary to the results obtained by ellipsometric measurements, dielectric measurements, and several other methods showing a significant dependence of $T_g$ on film thickness. The discrepancy is rather addressed to the method of assignment of the $T_g$ than to the actual location. In general, nanoscale PS objects demonstrate a pronounced broadening of the $T_g$ with decreasing film thickness. The broadening effect obviously causes a low-temperature shift of the beginning of the glass transition and, consequently, the $T_{g,\text{onset}}$ depression. For the ellipsometry technique and PS spin-coated films it is shown that $T_g$ assigned as the onset temperature of the expansivity temperature function demonstrates significant depression with decreasing thickness while the end point temperature of the glass transition, $T_{g,\text{end point}}$, remains almost constant. Since the nature of the assignment of Efrimovs technique is rather comparable with the assignment using the sensor position within the SThM technique, the absence of a surface layer with a lower $T_g$ may be explainable. In the earlier study,[15] where this surface layer has been detected, however, a polydisperse sample was investigated. Therefore, the existence of this layer may be connected also with the polydisperse nature of the sample. This point will be discussed again below.

Another interesting observation can be coupled to the data obtained while crossing over the $T_g$. The slope of the sensor signal changes dramatically due to the change in mechanical properties of the material under investigation; the sensor starts to penetrate the viscoelastic fluid present at temperatures above $T_g$. However, the slope of the penetration is different for the samples with different $M_w$, although the experimental conditions (tip size, surface roughness, etc.) were kept constant. The change in slope can now be attributed to the viscosity of the material above $T_g$.

The change in viscosity with respect to temperature can be calculated following the WLF equation:

$$\log\left(\frac{\eta}{\eta_{T_g}}\right) = -\frac{14.5(T - T_g)}{50.4 + (T - T_g)} \tag{2}$$

For a temperature difference of ≈80 K above $T_g$ will be the log $\eta \approx 4.16$; at temperatures 10 K above $T_g$ will be log $\eta \approx 10.6$.

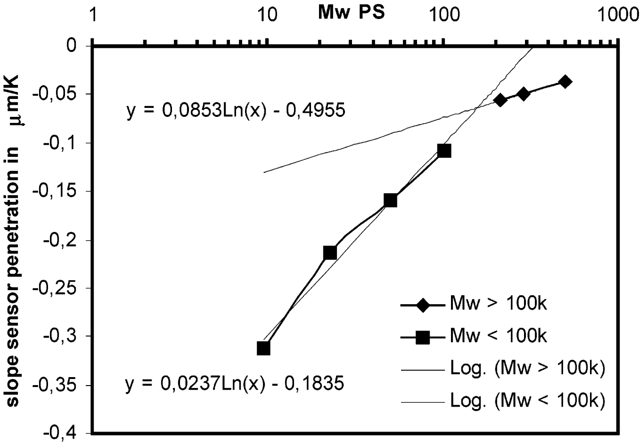

**Figure 4.** Plot of the slope of the sensor response after crossing $T_g$ with respect to molecular weight of the sample inspected by LTA. Two principle sets of data can be identified corresponding to two regimes of entangled molecules and nonentangled molecules. The crossover between the two regimes has been identified to occur at a molecular weight of approximately 116 kg/mol.

However, since the temperature dependency of the viscosity above $T_g$ follows in general an Arrhenius-type relationship

$$\eta \sim \exp(-E_a/kT) \tag{3}$$

and $E_a$ should be rather constant for the different samples of PS, the change in viscosity with temperature will be similar for all the polymers. Therefore, the main difference in thermomechanical behavior is a direct consequence of the differences in molecular weight $M$ as can be expressed by the relation

$$\eta \sim M^a \tag{4}$$

with $a = 1$ for molecular weights below a critical value and $a \sim 3.4$ (for PS) for molecular weights above the critical value. This critical value[1] is mainly dependent on the polymer structure (stiffness) and mobility. A very recent paper by Ding et al.[34] extensively discusses the question: When does a molecule become a polymer? The following conclusions were drawn:

Neither the average molecular weight between entanglement points $M_e$ (PS: $M_e = 17$ kg/mol) nor the Kuhn segment length (9 N for PS) is important for the location of the glass transition temperature $T_g$ but rather another empirical parameter that characterizes chain statistics: the molecular weight of random step in bead−spring model $m_R$ (for PS = 5.1K ∼ 50 monomers).

A molecule becomes a polymer (change from Rouse behavior to Gaussian coil) at a molecular weight $M_w \sim 10{-}20m_R$; this is for PS ∼ 100 kg/mol (1000 monomers).

Following this argumentation and the experimental evidence presented by Ding et al.,[34] only macromolecules with $M_w > 20m_R$ (for PS $M_w > 100$ kg/mol) will behave truly as polymers. This statement can be indeed supported by the experiments performed in this study. Two general regimes of viscoelastic behavior are clearly observable for the samples under investigation at temperatures above $T_g$. One group of samples, all samples with $M_w > 100$ kg/mol, show a rather moderate penetration of the sensor with increasing temperature. In contrast, the second group, the samples with 100 kg/mol $\geq M_w$, display a rather steep and immediate penetration of the sensor, typically for low viscous fluids, which show a Newtonian behavior. Santangelo and Roland[4] obtained a similar critical molecular weight result with respect to the fragility of PS. Below a degree of polymerization of roughly 1000 decreases the fragility of PS with decreasing molecular weight.

From the experimental data the slope of the intendation of the sensor with increasing temperatures can

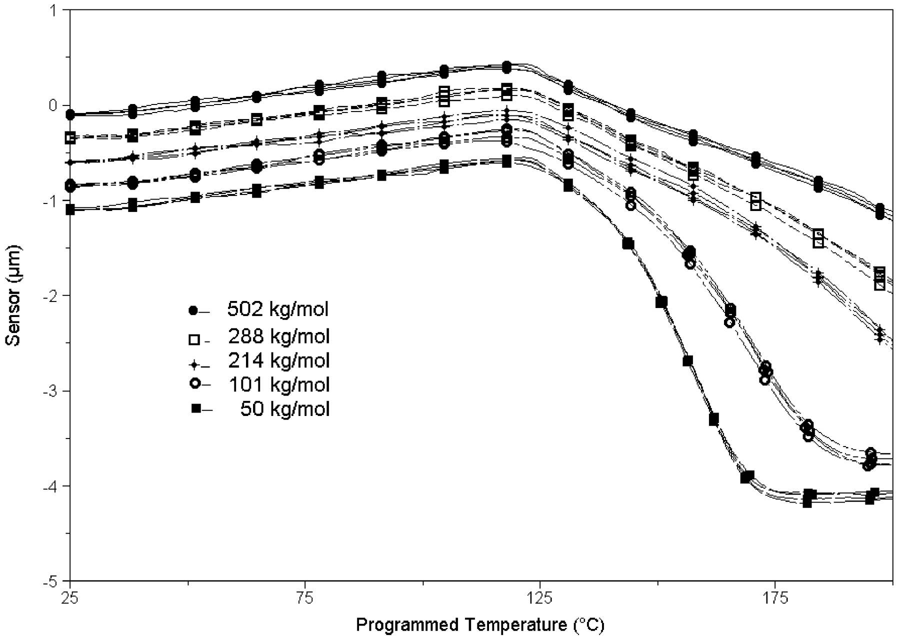

**Figure 5.** Results of the LTA experiments performed on surfaces of PS samples with different molecular weight using a smaller contact force than for the experiments depicted in Figure 3. Plotted is the respectively sensor position with respect to temperature. The samples with molecular weights of 50 and 101 kg/mol show at lower temperatures the behavior of entangled melts and at higher temperatures the behavior of nonentangled melts, whereas the samples with a molecular weight > 200 kg/mol show only the behavior of entangled melts. The first change in slope represents the $T_g$; the slope after crossing the $T_g$ can be related to the melt viscosity and thus the second change in slope for the samples with molecular weight 50 and 101 kg/ a change in behavior of an entangled melt to that of nonentangled melt. The samples with a molecular weight > 200 kg/mol show only the behavior of entangled melt.

be extracted and plotted against the $M_w$ (see Figure 4). Clearly both groups follow different regimes represented by the molecular characteristics of the samples under investigation. The data for both groups follow a logarithmic relation with respect to the $M_w$. The ratio between the two functions constructed from the data points originated from the two different groups is about 3.3, a value very close to the theoretical value of 3.4 as known for the exponential factor of the change of the viscosity dependency on the $M_w$ from below to above the critical $M_w$ for PS. The crossover between the two functions, and hence the change to polymer behavior, is at about 116 kg/mol located, again a value very close to the predicted ~100 kg/mol for the case of PS and in exceptional good agreement to the constant in the Flory−Fox equation. Changing the contact pressure to lower values (<30 nN), the picture becomes even clearer (see Figure 5).

Here, the two samples above the $M_e$ for PS ($M_w = 50$ and 101 kg/mol) display the two principal behaviors accounting for the entangled and the nonentangled regime. As the temperature increases, disentanglement in the small volume probed takes place, resulting in a change in penetration speed. Slopes for both regimes can be extracted again and are plotted in Figure 6.

Again, the crossover of both lines is slightly above 100 kg/mol (115 kg/mol) for the $M_w$ of PS. In general, the change of viscosity−$M_w$ dependency from the nonentangled to the entangled regime occurs at the critical molecular weight $M_c$ with $M_c \sim 2-4M_e$, thus for PS at about 60−80 kg/mol. This value obtained from macroscopic experiments comes close to the values for PS as shown by Ding et al.[34]

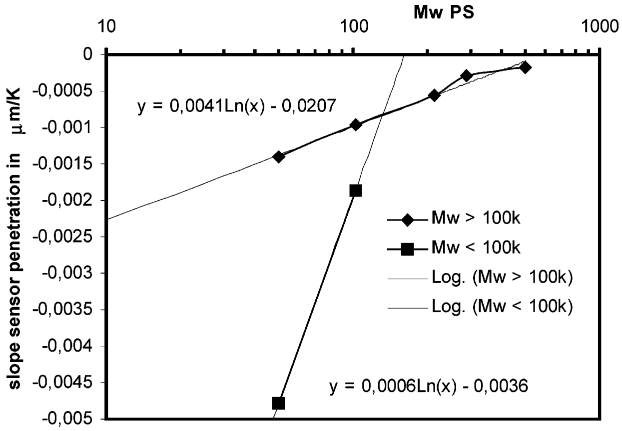

**Figure 6.** Plot of the slope of the sensor response after crossing $T_g$ with respect to molecular weight of the sample inspected by LTA using a smaller contact force than for the experiments described in Figures 3 and 4. The samples with molecular weights of 50 and 101 kg/mol show at lower temperatures the behavior of entangled melts and at higher temperatures the behavior of nonentangled melts, whereas the samples with a molecular weight > 200 kg/mol show only the behavior of entangled melts. The crossover between the two regimes of existence of melt, entangled molecules and nonentangled molecules has been identified to occur at a molecular weight of approximately 115 kg/mol.

Although the number of data points with respect to molecular weight is limited, and a more gradual change from the low molecular weight behavior to the high molecular weight behavior may be expected, one has to inspect more samples especially in the range between 100 and 200 kg/mol—the experiments on the monodisperse PS samples show a clear dependence of the thermomechanical behavior from the molecular weight that can be quantified. Therefore, this method may be useful for a determination of the molecular weight of an unknown sample, after proper calibration. To verify this possibility, a polydisperse sample of PS as used in the previous study[15] was studied again with respect to

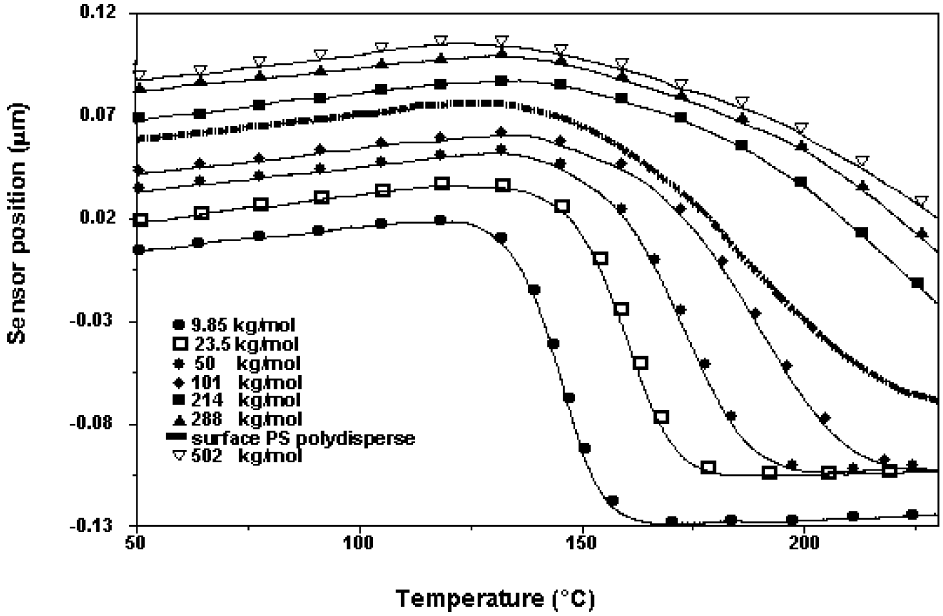

**Figure 7.** Results of the LTA experiments performed on surfaces of PS samples with different molecular weight together with a polydisperse sample of PS. Plotted is the sensor position with respect to temperature. The slope after crossing the $T_g$ can be related to the melt viscosity and thus used for determination of the molecular weight after calibration using samples of known molecular weight.

a quantitative analysis of the thermomechanical signal (see Figure 7).

The slope of the sensor penetration signal is clearly located between those of the samples of 101 and 214 kg/mol; the molecular weight has been determined to be ≈167 kg/mol following the function displayed in Figure 4, a value clearly between $M_n$ and $M_w$ of this sample. However, for samples with such polydispersity, an unambiguous determination of the molecular weight is rather questionable. There is very much a possibility of a surface enrichment of low molecular weight fractions, contributing to the lower $T_g$ at surfaces as described earlier by Kayiama,[13] but also by Russell.[35] Both observed that lower molecular weight fractions display a lower surface tension and in summary a decrease in free energy when located at surfaces due to smaller changes in conformational entropy. These effects drive them to the surface and initiate a phase separation in terms of molecular weight. The resulting surface layer will display a lower glass transition according to the already above-mentioned Flory−Fox equation. In our earlier study[15] a polydisperse sample was investigated showing a thin surface layer with reduced $T_g$, which can now attributed to an enrichment of lower molecular weight fractions at the surface. The molecular weight value determined for the surface of the polydisperse sample may be larger than one would expect ($M_n$ or even smaller), providing the underlying explanation is correct. In the moment, the only explanation possible is connected with time scales needed for the demixing of the macromolecules with respect to their molecular weight and to the corresponding surface tensions. Those time scales may by far exceed the annealing times used for the preparation of the sample.

## Conclusions

The inspection of the thermal properties of PS samples with a molecular weight spanning from 9.85 to 502 kg/mol and a very narrow molecular weight distribution using an AFM equipped with a thermal probe in the local thermal analysis (LTA) resulted in new data concerning the properties of the thin surface layer of glassy polymers. No difference in $T_g$ at the very surfaces could be detected for the investigated PS samples. It is concluded that the lower $T_g$ on the surface of glassy polymers as detected for polydisperse samples is generated rather by demixing of macromolecules with respect to their molecular weight than by enrichment of chain ends close to the surface.

Instead, different molecular weights contribute to differences in the micro-thermomechanical behavior. It is possible to discriminate between entangled and nonentangled regimes due to the differences in micromelt rheology. A careful analysis hints to possibilities to use this analytic method for the determination of $M_w$ on and of polymeric surfaces. With the a careful calibration of the dependency of the LTA (TMA) signal onto molecular weight of inspected samples, there are new possibilities to analyze on micron scale molecular characteristics such as $M_w$, viscosity, etc., for complex polymeric systems such as polycondensates (polyesters, polyamides) but also for thermosets and even perhaps to estimate cross-link densities, etc.

Furthermore, hints to a disentanglement of macromolecules with molecular weights lower than the critical molecular weight to form a random coil, initiated by the indentation with the thermal probe during the LTA experiment, are found. In the case of PS as a polymer with bulky side groups the intermolecular cooperativity is enhanced and results in a relatively high $T_g$, and one that is more molecular weight dependent. Therefore, it is possible to use this method to discriminate with a sufficient sensitivity between the different regimes of (macro)molecular behavior.

## References and Notes

(1) Brandrup, J., Immergut, E. H., Eds.; *Polymer Handbook*, 3rd ed.; Wiley: New York, 1989.

(2) Ge, S.; Pu, Y.; Zhang, W.; Rafailovich, M.; Sokolov, J.; Buenviaje, C.; Buckmaster, R.; Overney, R. M. *Phys. Rev. Lett.* **2000**, *85*, 2340.

(3) Tanaka, K.; Taura, A.; Ge, S.-R.; Takahara, A.; Kajiyama, T. *Macromolecules* **1996**, *29*, 3040.
(4) Santangelo, P. G.; Roland, C. M. *Macromolecules* **1998**, *31*, 4581.
(5) Jones, R. A. L. *Nat. Mater.* **2003**, *2*, 645.
(6) Mattsson, J.; Forrest, J. A.; Börjesson, L. *Phys. Rev. E* **2000**, *62*, 5187.
(7) de Gennes, P. G. *Eur. Phys. J.* **2000**, *E2*, 201.
(8) van der Veen, J. F. *Surf. Sci.* **1999**, *433–435*, 1.
(9) Wallace, W. E.; Fischer, D. A.; Efimenko, K.; Wu, W.; Genzer, J. *Macromolecules* **2001**, *34*, 5081.
(10) van der Gucht, J.; Besseling, N. A. M.; Fleer, G. J. *Macromolecules* **2002**, *35*, 6732.
(11) Bliznyuk, V. N.; Assender, H. E.; Briggs, G. A. D. *Macromolecules* **2002**, *35*, 6613.
(12) Pu, Y.; Ge, S.; Rafailovich, M.; Sokolov, J.; Duan, Y.; Pearce, E.; Zaitsev, V.; Schwarz, S. *Langmuir* **2001**, *17*, 5865.
(13) Tanaka, K.; Kajiyama, T.; Takahara, A.; Tasaki, S. *Macromolecules* **2002**, *35*, 4702.
(14) Johannsmann, D. *Eur. Phys. J. E.* **2002**, *8*, 257.
(15) Fischer, H. *Macromolecules* **2002**, *35*, 3592.
(16) Freyer, D. S.; Nealey, P. F.; de Pablo, J. J. *Macromolecules* **2000**, *33*, 6439.
(17) Keddie, J. L.; Jones, R. A. L. *Isr. J. Chem.* **1995**, *35*, 21.
(18) Tsui, O. K. C.; Zhang, H. F. *Macromolecules* **2001**, *34*, 9139.
(19) Xie, F.; Zhang, H. F.; Lee, F. K.; Du, B.; Tsui, O. K. C.; Yokoe, Y.; Tanaka, K.; Takahara, A.; Kajiyama, T.; He, T. *Macromolecules* **2002**, *35*, 1491.
(20) Forrest, J. A.; Mattsson, J. *Phys. Rev. E.* **2000**, *61*, R53.
(21) Mattsson, J.; Forrest, J. A.; Börjesson, L. *Phys. Rev. E* **2000**, *62*, 5187.
(22) de Maggio, G. B.; Frieze, W. E.; Gidley, D. W.; Zhu, M.; Hristov, H. A.; Yee, A. F. *Phys. Rev. Lett.* **1998**, *58*, R1223.
(23) Kawaguchi, D.; Tanaka, K.; Kajiyama, T.; Takahara, A.; Tasaki, S. *Macromolecules* **2003**, *36*, 1235.
(24) Kajiyama, T.; Tanaka, K.; Takahara, A. *Macromolecules* **1997**, *30*, 280.
(25) Kajiyama, T.; Tanaka, K.; Takahara, A. *J. Polym. Sci., Polym. Chem.* **2004**, *42*, 639.
(26) Hammerschmidt, J. A.; Gladfelter, W. L.; Haugstad, G. *Macromolecules* **1999**, *32*, 3360.
(27) Akabori, K.; Tanaka, K.; Kajiyama, T.; Takahara, A. *Macromolecules* **2003**, *36*, 4937.
(28) Mansfield, K. F.; Theodoru, D. N. *Macromolecules* **1991**, *24*, 6283.
(29) Baschnagel, J.; Binder, K. *J. Phys. I* **1996**, *6*, 1271.
(30) Breuer, H.; Rehage, G. *Kolloid-Z.* **1967**, *216/217*.
(31) Pollock, H. M.; Hammiche, A. *J. Phys. D: Appl. Phys.* **2001**, *34*, R23.
(32) Slough, C. G. Characteristics of $T_g$ Detection Using Micro-Thermomechanical Analysis, TA Analytical note 277. Blaine, R. L.; Slough, C. G.; Price, D. M.; Proceedings of the 27th Conference of the North American Thermal Analysis Society, Sept. 20–22, 1999, Savannah, GA, Micro-thermal-analysis, Calibration, Repeatability and Reproducibility.
(33) Efremov, M. Y.; Olson, E. A.; Zhang, M.; Zhang, Z.; Allen, L. H. *Macromolecules* **2004**, *37*, 4607.
(34) Ding, Y.; Kisliuk, A.; Sokolov, A. P. *Macromolecules* **2004**, *37*, 161.
(35) Kerle, T.; Lin, Z.; Russel, T. P. *Macromolecules* **2001**, *34*, 3438.

MA048376A